

THE OFFICIAL MAGAZINE OF THE OCEANOGRAPHY SOCIETY

# Oceanography

## CITATION

Gordon, A.L., E.L. Shroyer, A. Mahadevan, D. Sengupta, and M. Freilich. 2016. Bay of Bengal: 2013 northeast monsoon upper-ocean circulation. *Oceanography* 29(2):82–91, <http://dx.doi.org/10.5670/oceanog.2016.41>.

## DOI

<http://dx.doi.org/10.5670/oceanog.2016.41>

## COPYRIGHT

This article has been published in *Oceanography*, Volume 29, Number 2, a quarterly journal of The Oceanography Society. Copyright 2016 by The Oceanography Society. All rights reserved.

## USAGE

Permission is granted to copy this article for use in teaching and research. Republication, systematic reproduction, or collective redistribution of any portion of this article by photocopy machine, reposting, or other means is permitted only with the approval of The Oceanography Society. Send all correspondence to: [info@tos.org](mailto:info@tos.org) or The Oceanography Society, PO Box 1931, Rockville, MD 20849-1931, USA.

# Bay of Bengal

## 2013 Northeast Monsoon Upper-Ocean Circulation

By Arnold L. Gordon, Emily L. Shroyer, Amala Mahadevan,  
Debasis Sengupta, and Mara Freilich



Photo credit: San Nguyen

“ The observations obtained from R/V *Revelle* in November and December 2013 reveal a complex array of energetic mesoscale and submesoscale features, complete with swirls and fronts of contrasting temperature and salinity, as well as an ITE that obscures the regional pattern of the Bay of Bengal as visualized by Argo-based climatology. ”

**ABSTRACT.** The upper 200 m of the two northern Indian Ocean embayments, the Bay of Bengal (BoB) and the Arabian Sea (AS), differ sharply in their salinity stratification, as the Asian monsoon injects massive amounts of freshwater into the BoB while removing freshwater via evaporation from the AS. The ocean circulation transfers salt from the AS to the BoB and exports freshwater from the BoB to mitigate the salinity difference and reach a quasi-steady state, albeit with strong seasonality. An energetic field of mesoscale features and an intrathermocline eddy was observed within the BoB during the R/V *Revelle* November and December 2013 Air-Sea Interactions Regional Initiative cruises, marking the early northeast monsoon phase. Mesoscale features, which display a surprisingly large thermohaline range within their confines, obscure the regional surface water and thermohaline stratification patterns, as observed by satellite and Argo profilers. Ocean processes blend the fresh and salty features along and across density surfaces, influencing sea surface temperature and air-sea flux. Comparing the *Revelle* observations to the Argo data reveals a general westward migration of mesoscale features across the BoB.

## INTRODUCTION

The ocean and the atmosphere, linked by air-sea exchange, together shape the climate and its response to external factors. While the atmosphere envelops the globe, the ocean is confined within basins of varied dimensions. Although these basins have a degree of connectivity that enables interocean exchange, each ocean has its own unique temperature and salinity patterns and its own unique role in the climate system (Gordon, 2001; Sprintall et al., 2013). The relatively warm and salty Atlantic and the cooler and fresher Pacific stretch from the high latitudes of each hemisphere, while the Indian Ocean, blocked by the Asian continent,

has limited extent north of the equator.

The two northern Indian Ocean embayments, the Bay of Bengal (BoB) and the Arabian Sea (AS), are strikingly different from one another despite their close proximity; the BoB receives an excess of freshwater, while the AS is subject to excess evaporation. Both are strongly coupled to the Asian monsoon system. Consequentially, the BoB surface layer differs markedly from that of the AS, since the contrasting surface fluxes are not fully compensated by ocean circulation. This contrast is well brought out by the World Ocean Circulation Experiment (WOCE) Indian Ocean 1995 IO1 section near 9°N (Figure 1). In the

surface layer, the difference between BoB and AS salinity is 5 psu, similar to the maximum sea surface salinity (SSS) difference found elsewhere over the entire world ocean. In recent decades, the BoB has been freshening, while the AS has become saltier, possibly a consequence of intensification of the hydrological cycle (Durack and Wijffels, 2010), or a decrease in freshwater exchange between the BoB and the AS.

Ocean circulation maintains quasi-stationary conditions by moving low-salinity upper-ocean water from the BoB to the AS via the East Indian Coastal Current (EICC), which runs along the western margin of the BoB and around the southern rim of Sri Lanka, and through engagement with the larger-scale network of currents involving the tropical circulation (Schott and McCreary, 2001; Shankar et al., 2002; Sengupta et al., 2006; Schott et al. 2009; Wijesekera et al. 2015; Jensen et al., 2016, in this issue). Salty AS water is advected to the BoB within the thermocline. These exchanges are affected by the reversing monsoon wind patterns. The efficiency of the BoB/AS exchange, which no doubt varies not just seasonally but also interannually and at longer periods, determines the thermohaline stratification contrast between these two northern Indian Ocean embayments.

## BAY OF BENGAL REGIONAL OCEANOGRAPHY OVERVIEW

The Air-Sea Interactions Regional Initiative (ASIRI) in the northern Indian Ocean aims to understand and quantify the coupled atmosphere-ocean dynamics of the BoB with relevance to Indian Ocean monsoons (Sengupta et al., 2016; Wijesekera et al., in press). As part of ASIRI, two research cruises were conducted from R/V *Roger Revelle* in the BoB during November and December 2013 (Figure 2).

November and December fall within the early stages of the northeast monsoon when the winds blow cool dry air over the BoB from the northeast, with mean speeds of  $\sim 6 \text{ m s}^{-1}$  (Varkey et al., 1996), leading to a wind stress increase from  $0.02 \text{ N m}^{-2}$  in November to  $0.1 \text{ N m}^{-2}$  in January (Schott et al., 2009), consistent with the wind recorded during the *Revelle* cruises. The November to December timeframe marks the ocean spin-up

to the developing northeast monsoon, which replaces the summer monsoon forcing. Tropical cyclones are common in the late summer and transition to the northeast winter monsoon. During Leg 2 between December 5 and 8, 2013, the wind stress recorded on the ship reached  $0.4 \text{ N m}^{-2}$ , with a wind speed as high as 33 knots, a result of Tropical Cyclone Madi to the northwest.

The November to December timeframe is after the freshet of the major rivers that flow into the Bay of Bengal, with maximum discharge toward the end of the summer monsoon. Sengupta et al. (2006) report that the annual runoff into the Bay of Bengal is  $2,950 \text{ km}^3$ , or  $0.094 \text{ Sv}$  ( $1 \text{ Sv} = 1 \times 10^6 \text{ m}^3 \text{ s}^{-1}$ ), more than 50% of the freshwater runoff into the entire tropical Indian Ocean. Spread out over the BoB area of  $2.17 \times 10^{12} \text{ m}^2$  (including the Andaman Sea), it yields a net input of  $1.34 \text{ m yr}^{-1}$  of river discharge. The Ganges and Brahmaputra

Rivers together account for 25% of the total freshwater inflow into the BoB (Papa et al., 2010), with the summer monsoon accounting for nearly 70% of the annual discharge. Sengupta et al. (2006) find the annual precipitation over the BoB to be  $4,700 \text{ km}^3$  that, when spread over the BoB area, yields  $2.16 \text{ m yr}^{-1}$ , and the annual evaporation to be  $3,600 \text{ km}^3$  ( $1.66 \text{ m yr}^{-1}$ ), yielding P-E of  $\sim 0.5 \text{ m yr}^{-1}$ . Combined with the river runoff into the BoB, the net annual freshwater input due to P-E+R is  $1.84 \text{ m yr}^{-1}$ . Earlier estimates by Varkey et al. (1996; from their Tables 2 and 3) find similar net precipitation as Sengupta et al. (2006) but a much lower evaporation rate of  $0.34 \text{ m yr}^{-1}$ , resulting in a much larger net P-E+R of  $3.1 \text{ m yr}^{-1}$ .

The massive input of freshwater results in low salinity of the upper-ocean layer with a strong surface barrier layer stratification (Shetye et al., 1996; Vinayachandran et al., 2002). Pant et al. (2015) find that SSS in the interior

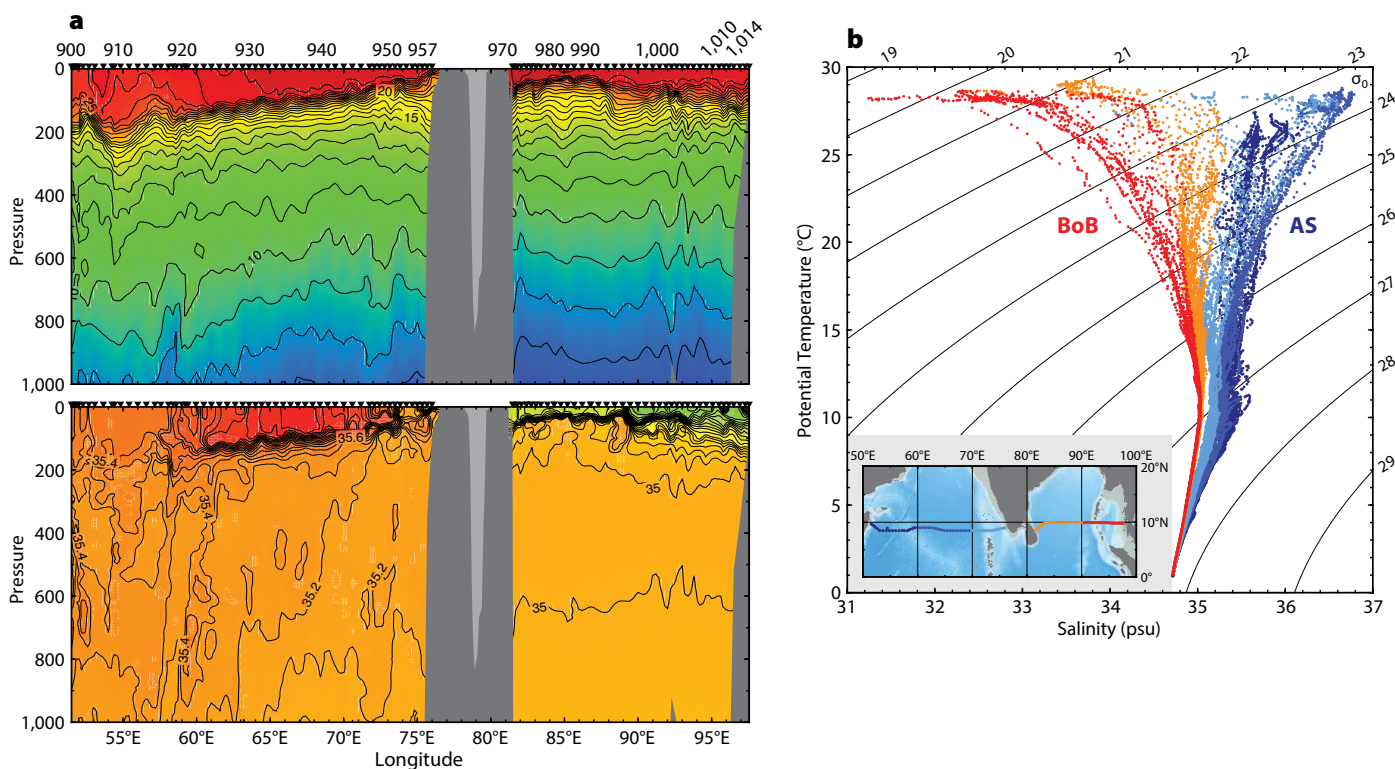


**FIGURE 1.** (a) The World Ocean Circulation Experiment (WOCE) I01 is a zonal section that cuts across the Bay of Bengal (data obtained in October 1995) and the Arabian Sea (data obtained in September 1995) at 9°N. Potential temperature (upper panel) and salinity (lower panel) are shown for the upper 1,000 m. (b) Potential temperature versus salinity color-coded by longitude (see map insert). The Bay of Bengal/Arabian Sea (BoB/AS) contrast sharply in the thermocline and surface layer,  $>10^\circ\text{C}$ ; smaller differences are found in the lower thermocline and intermediate layers near  $4^\circ\text{C}$ . The particularly sharp contrast between these two northern embayments of the Indian Ocean is apparent at high temperatures ( $>25^\circ\text{C}$ ).

BoB reflects local freshwater forcing during the summer, whereas in winter it is governed more strongly by horizontal advection of riverine-origin water. SSS variability at interannual time scales responds more to the Indian Ocean Dipole (IOD)—a positive IOD leading to lower SSS—than to the El Niño-Southern Oscillation (ENSO). The relatively salty water derived from the Arabian Sea, spreading beneath the surface barrier layer as a salinity maximum ( $S_{max}$ ), mixes into the surface water to counter the massive summer freshwater inflow (Vinayachandran et al., 2013; Akhil et al., 2014; Wilson and Riser, 2016). Spreading of the saline water along isopycnals toward the northern Bay of Bengal may also play a role in mixing of the salty and relatively fresh waters (Rao and Sivakumar, 2003).

During the northeast monsoon, the EICC flows southward, with westward flow along the southern rim of Sri Lanka

(Schott and McCready, 2001; Schott et al. 2009). EICC seasonality does not scale exactly with monsoon forcing. Shetye et al. (1996), using ship drift data, show a well-developed southward-flowing EICC in November and December that weakens in January and reverses in February. Using observations from December 1991, Shetye et al. (1991, 1996) conclude that the EICC is driven by winds along the Indian coast as well as Ekman-induced upwelling in the western BoB. Durand et al. (2009) detail the complex interaction of the EICC with offshore currents. They state that the EICC is discontinuous, with recirculating loops along its path. Pant et al. (2015) also describe a southward-flowing EICC from October to December, giving way to northward flow from January to March. The variable southward EICC transport has an impact on the ponding of the river discharge into the northern BoB (Pant et al., 2015). During a positive IOD, as the EICC

weakens or disappears, the freshwater of the northern Bay of Bengal is exported along the eastern margin of the bay (see Pant et al., 2015, Figure 12; this may also happen but to a lesser extent during negative IOD—see their Figure 11). The IOD was mostly negative in 2013–2014, albeit slightly positive in late 2013, which may suggest a stronger EICC during the 2013 *Revelle* cruises. Consistent with this observation, Wijesekera et al. (2015) show strong southward-flowing EICC from October through December 2013, feeding into westward surface flow along the southern rim of Sri Lanka.

The enormous amount of freshwater entering the BoB is removed via two pathways: around the southern rim of Sri Lanka and along the eastern margin of the BoB. Pant et al. (2015) find that at times, the northern BoB freshwater pool is advected southward within the eastern BoB. Sengupta et al. (2006) propose that BoB river freshwater export

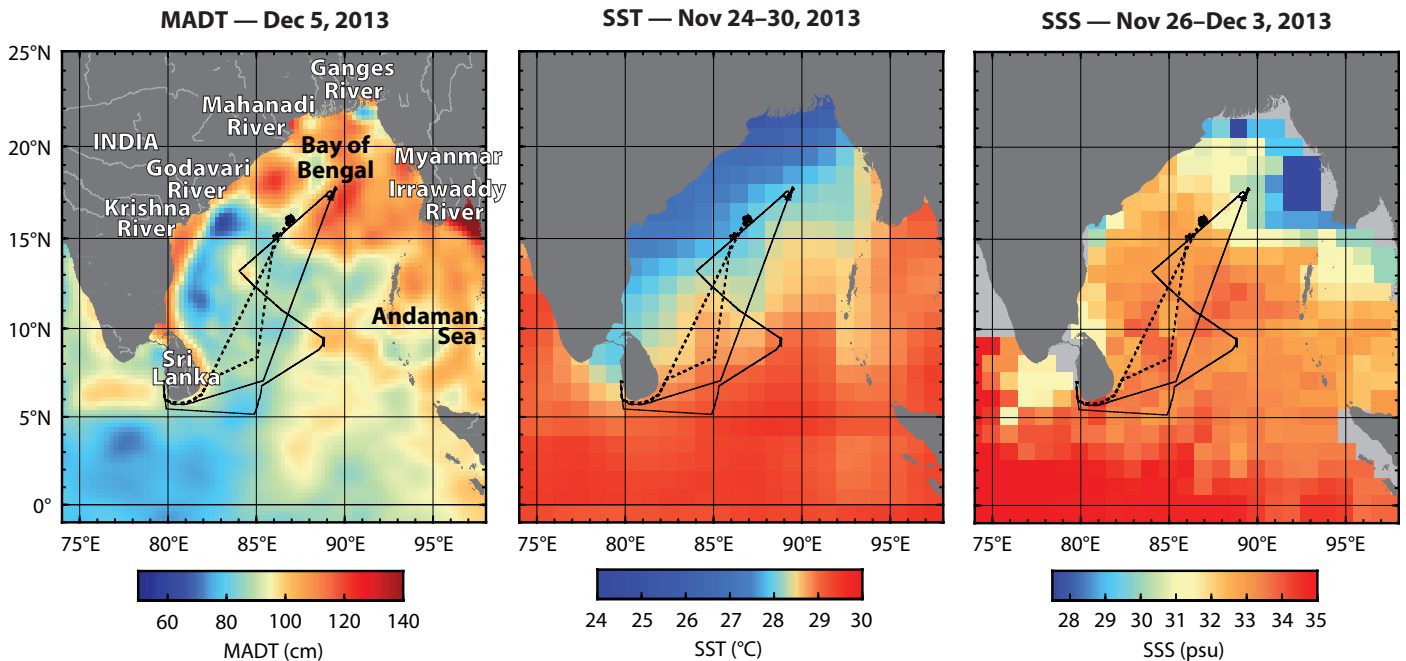


**FIGURE 2.** The two legs (Leg 1 dashed; Leg 2 solid) of the 2013 Air-Sea Interactions Regional Initiative (ASIRI) cruise in the Bay of Bengal. (left) Mean Absolute Dynamic Topography (MADT; <http://www.aviso.altimetry.fr/en/data/product-information/citation-and-aviso-products-licence.html>) (center) Sea surface temperature (SST; Reynolds et al., 2007; <http://www.esrl.noaa.gov/psd/data/gridded/data.noaa.oisst.v2.html>). (right) Aquarius satellite version 4 of sea surface salinity (SSS; Lagerloef et al., 2008; <http://aquarius.nasa.gov>).

along the eastern margin crosses the equator and turns westward upon meeting the Indonesian Throughflow near 10°S. It then spreads across the southern tropical Indian Ocean within the South Equatorial Current to eventually reach into the Arabian Sea. Aquarius satellite SSS data suggest that BoB outflow along its eastern boundary reaches across the equator, flowing along the southern coast of Java before turning westward with the South Equatorial Current along with the Indonesian Throughflow plume. Upon reaching the western margin of the Indian Ocean, some of this water turns northward to supply relatively low-salinity upper-ocean water to the Arabian Sea. In addition, there is a monsoonal reversing flow along the southern rim of Sri Lanka, which is an explicit research element in the ASIRI project as well as in the Northern Arabian Sea Circulation–autonomous research (NASCar) program (Wijesekera et al., in

press). Which pathway, western or eastern BoB, dominates on an annual basis? The eastern path is year-round; the western path, tracking along the southern rim of Sri Lanka, is highly seasonal. The NASCar program will investigate the freshwater input to the AS.

### ANALYSIS Surface Water

Figure 2 shows November and December 2013 sea surface height (SSH), sea surface temperature (SST), and SSS for the Bay of Bengal. During that period, the southwestern BoB displays the lowest SSH, the northwestern BoB has the coldest SST of ~24°C, and the northeastern sector, where the Ganges-Brahmaputra and Irrawaddy Rivers discharge their freshwater, generally shows the lowest SSS of less than 28 psu. The Aquarius satellite data do not resolve SSS near coastal regions (shown as gray boxes in Figure 2), where the close proximity to land leads to

SSS well below 28 psu.

The in situ SSS color-coded surface layer circulation and the SST/SSS scatter further reveal the diversity of features observed during R/V *Revelle* 2013 cruises (Figure 3). SSS gradients and complex surface layer currents along *Revelle*'s track largely reflect energetic mesoscale features. Comparison of SST/SSS scatter from the ship's underway surface layer temperature and salinity system (thermosalinograph) with the Reynolds and Aquarius views of the entire BoB suggests that data for the “L2 northern feature” (see Figures 2 and 4) fit the surface water from east of the Leg 2 track more closely. The Ocean Surface Current Analyses (OSCAR; Bonjean and Lagerloef, 2002) for mid-December 2013 show a distinct westward flow near 15°N emanating from the eastern BoB sector that then curls to the north near 88°E, consistent with the ship-based acoustic Doppler current profiler vectors at the L2 northern feature.

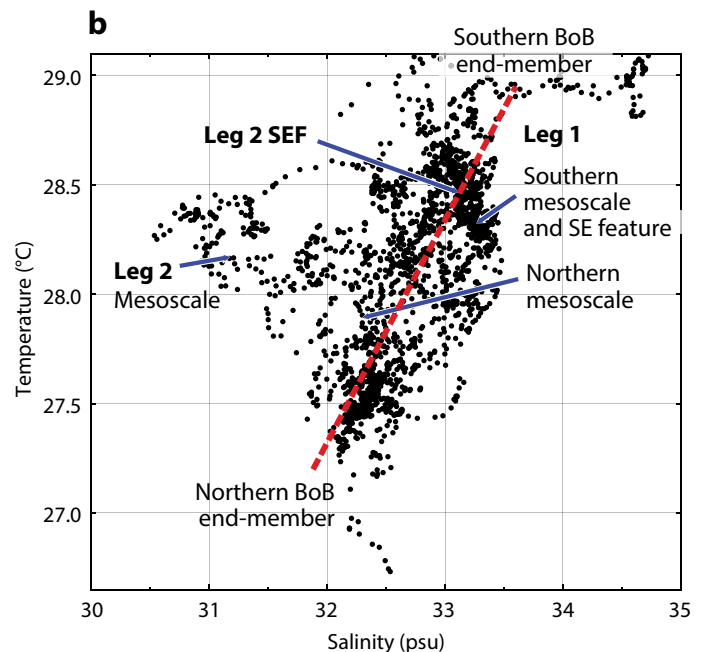
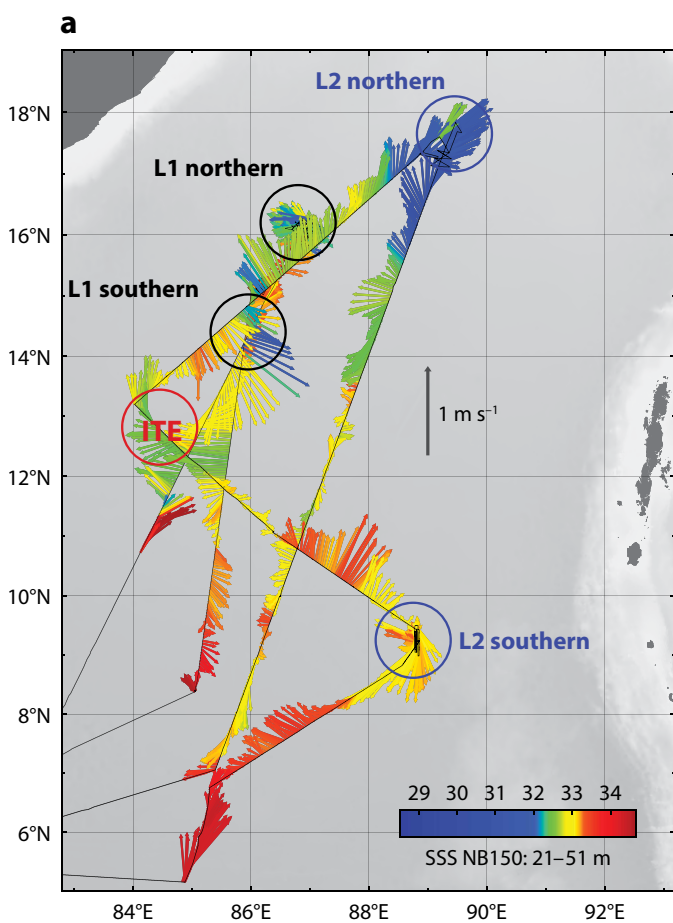


**FIGURE 3.** (a) The tracks of R/V *Revelle* Legs 1 and 2 with ship-hull acoustic Doppler current profiler (ADCP) measured current between 21 m and 51 m depth, color-coded by sea surface salinity. The circles denote mesoscale surveys, which are discussed in the text. The intrathermocline eddy (ITE) observed on Leg 2 is also discussed in the main text. (b) SST/SSS scatter from the November–December 2013 R/V *Revelle* thermosalinograph. Dashed red line: approximate north-south SST/SSS trend. The blue arrows indicate the T/S positions of mesoscale features shown in (a).

Taken together, these observations suggest that the low SSS at this feature has origins in the northeast BoB. Data from the Leg 1 northern and southern surveys fall closer to the main SST/SSS scatter that stretches between the northern and southern BoB and hence are not associated with significant zonal flow.

A Hovmöller diagram based on satellite altimeter SSH data (Figure 4) also reveals westward propagation of SSH features from the eastern BoB at a rate of  $6.2 \text{ cm s}^{-1}$ . Westward propagation was noted by Yu et al. (1991), who say: “Those wind-generated Kelvin waves efficiently transmit the wind input energy to the eastern boundary of the Bay of Bengal, where long Rossby waves further radiate some of the energy to the interior of the bay.” Using OSCAR velocities, the SSS observations from Leg 2 are traced backward to their origin (Figure 5). For the most part, the mesoscale flow field transported the observed SSS features from regions to the east of the *Revelle* track with some transport from the northwest in the northwestern part of the ship track. The low-salinity surface water observed at the northern end (L2 northern) traces back to the Irrawaddy River, with an average advective rate of about  $10 \text{ cm s}^{-1}$  during October and November, consistent with the observed westward propagation of mesoscale SSH features (Figure 4).

### Temperature and Salinity Stratification

Argo float coverage since 2003 provides a “climatological” view along the BoB’s meridional spine (Figure 6a). Relatively salty water near 100 m depth in the southern BoB, particularly during the summer monsoon, is drawn from the AS with the Summer Monsoon Current (SMC; Vinayachandran et al., 1999; Jensen, 2001). The  $S_{\text{max}}$  is not continuous within BoB, but is observed as isolated pockets (Sastry et al., 1985), dissected by energetic mesoscale activity. The IIOE Indian Ocean atlas (Wyrтки, 1971) does not show the shallow  $S_{\text{max}}$  core layer as entering the Bay of Bengal; it is suspected

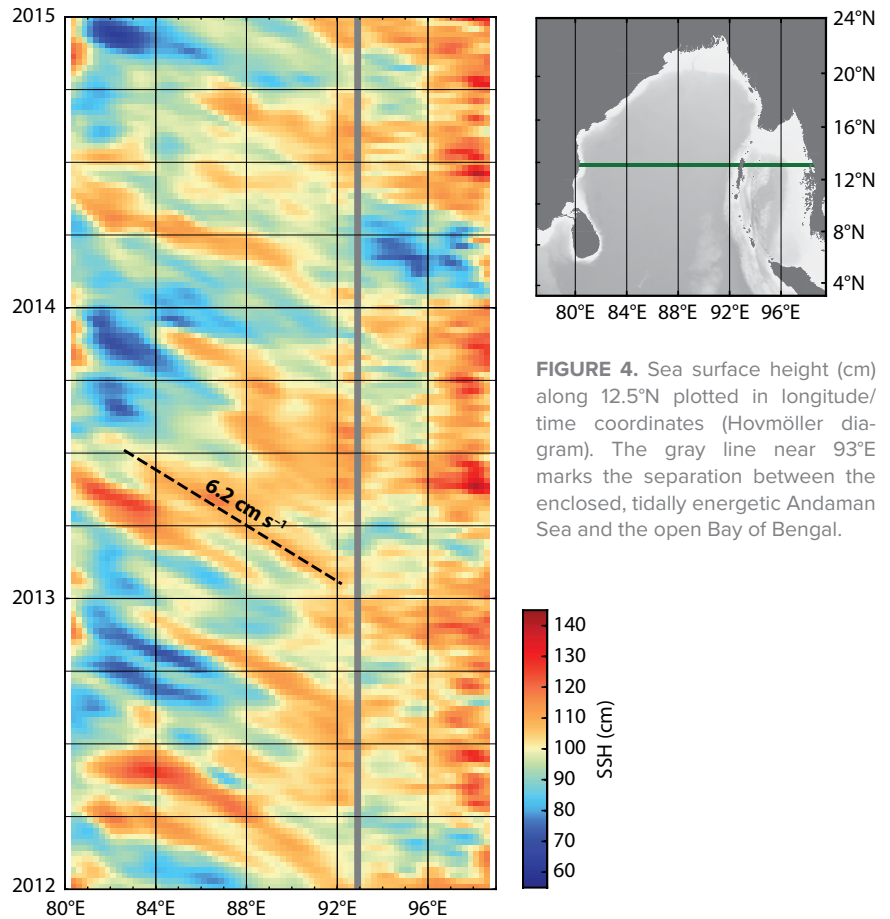


**FIGURE 4.** Sea surface height (cm) along  $12.5^\circ\text{N}$  plotted in longitude/time coordinates (Hovmöller diagram). The gray line near  $93^\circ\text{E}$  marks the separation between the enclosed, tidally energetic Andaman Sea and the open Bay of Bengal.

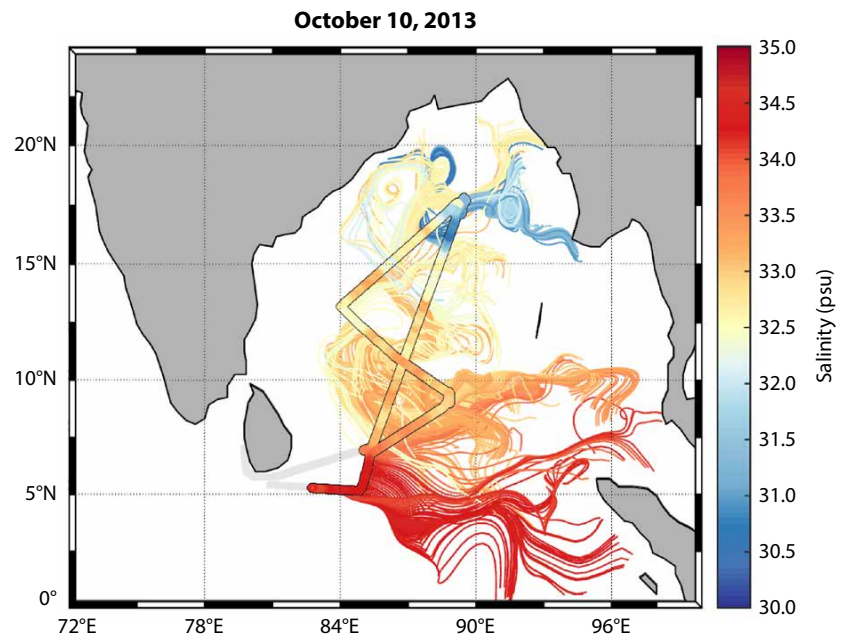


**FIGURE 5.** SSS measurements from R/V *Revelle* Leg 2 are advected back in time to October 10, 2013, using Ocean Surface Current Analyses (OSCAR) sea surface currents. Color indicates salinity (psu). Lines show the trajectory between the inferred location on October 10, 2013, and the ship transit for every hundredth SSS measurement. SSS measurements are shown on the ship track and are outlined in black.

that the eddies were not well captured by the BoB sections. Vinayachandran et al. (2013) suggest that upwelling along meanders of the SMC associated with intraseasonal wind events enable the salty Arabian Sea water to mix with the surface layer, compensating for the excess of freshwater due to precipitation plus run-off excess over evaporation. In addition, the occurrence of along-isopycnal salinity gradients (Figure 6a) indicate that isopycnal mixing processes, perhaps associated with mesoscale dynamics, may also play a role in mixing the AS salty inflow into the relatively fresh surface layer of the BoB. The processes that govern the mixing of the salty and fresh waters have a direct impact on upper-ocean stratification and thereby can influence air-sea exchange; these connections are a central topic of ASIRI.

The T/S scatter of the Argo meridional section for the two monsoon seasons (Figure 6b) reveals significant seasonality at  $\sigma_0$  values less than 23 (upper

75 m), in addition to the Arabian Sea  $S_{\max}$  feature near 100 m depth. In winter, the surface layer cools with decreasing salinity as the sea surface is approached, reflecting winter conditions within the northern BoB and the warmer low-latitude waters. In summer, the low-salinity upper 50 m of the water column are uniformly warm,  $>28^\circ\text{C}$ , the threshold commonly used to indicate atmospheric convection (Gadgil et al., 1984). WOCE section I9n (Talley, 2013), January 24 to March 5, 1995, obtained conductivity-temperature-depth (CTD) data on the Myanmar continental shelf, where the winter-cooled shelf water was observed spreading offshore at  $\sim 50$  m depth as a  $T_{\min}$  of  $24^\circ\text{C}$  to  $25^\circ\text{C}$ . This subduction process might occur elsewhere along the northern margins of the BoB during the winter, and may prove to be an important means of ventilating the upper thermocline. The Argo T/S reveal a low-salinity feature in the  $\sim 18^\circ\text{C}$  to  $26^\circ\text{C}$  layer, which is similar to the intrathermocline eddy

(ITE) observed on Leg 2, discussed below.

The meridional temperature and salinity sections constructed from Leg 2 of the *Revelle* cruises (Figure 7a) reveal the deepening of the isopycnals under the thicker low-salinity surface layer of the northern BoB. Decreasing salinity with increasing latitude is evident on the 21, 22, and 23  $\sigma_0$  surfaces. The  $\sigma_0$  24 surface, which is generally below 100 m depth, reveals minor salinity change. The jagged fluctuations of  $<50$  km scale represent mesoscale features (Figure 7b), amounting to up to 0.5 in salinity on the  $\sigma_0$  surfaces, which may be a product of stirring waters of contrasting salinity along isopycnals.

### Mesoscale Surveys Relative to Regional T/S

The dynamics of the mesoscale surveys during the *Revelle* cruise are the subject of detailed ASIRI data analysis. Here, we discuss three features: L1 northern, L2 southern, and ITE (Figure 3a). The T/S scatter of L2 southern and L1 northern

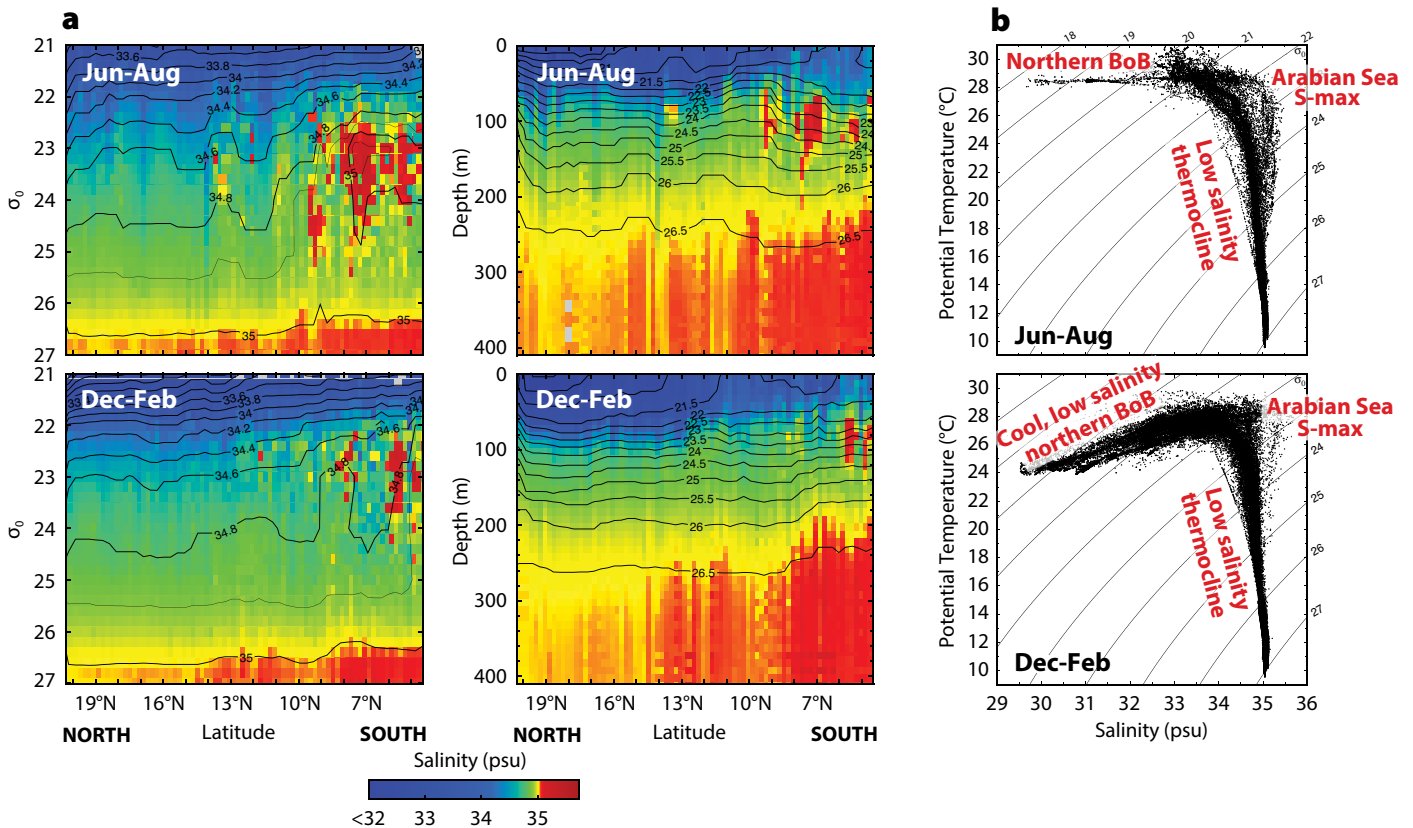


**FIGURE 6.** (a) Argo 2003–2014 profiles reveal the climatological thermohaline stratification along the meridional “spine” of the Bay of Bengal. The right panels show the salinity field, with isopycnals as black contours. The left panels show the  $\sigma_0$  field, with salinity as black contours. December-February and June-August periods are shown to denote the monsoon effect. (b) T/S of the Argo data shown in (a).



(Figure 8a and b, respectively) encompass a significant percentage of the full T/S range observed by the 2013 *Revelle* cruise (which matches nearly the full T/S range of the entire BoB Argo T/S scatter, not shown). The L2 southern near 8.6°N, displays strong presence of an  $S_{\max}$  of 35.2, a clear signature of an AS intrusion. A secondary  $S_{\max}$  is observed near 18°C, which also likely derived from the AS. A broad  $S_{\min}$  of 34.7 spans the layer between the two  $S_{\max}$  cores, which is also apparent in the Argo section (Figure 6) south of 10°N.

The L1 northern feature (Figure 8b) at 16°N displays a weaker, attenuated AS  $S_{\max}$  of 34.8, which falls in the same  $\sigma_0$  range,  $\sim 23$ , as the  $S_{\max}$  of L2 southern, a product of isopycnal mixing. L1 northern displays two T/S clusters within the 23°C to 27°C thermocline interval. The fresher T/S cluster matches water types of the northwest BoB observed by the Argo profiles (not shown), perhaps associated with the interaction between the EICC with the interior flow, as postulated by Durand et al. (2009).

### Intrathermocline Eddy

During Leg 2, the underway CTD recorded an ITE that is marked in the T/S scatter shown in Figure 8a. As first noted by Dugan et al. (1982), ITE structures are characterized by a subsurface lens of relatively homogeneous water that spans 10–100 km in diameter, and has a vertical extent on the order of 100 m. The lens divides the normal thermocline stratification, with the upper thermocline forming a dome (cyclonic shear) over the top of the lens, and the lower

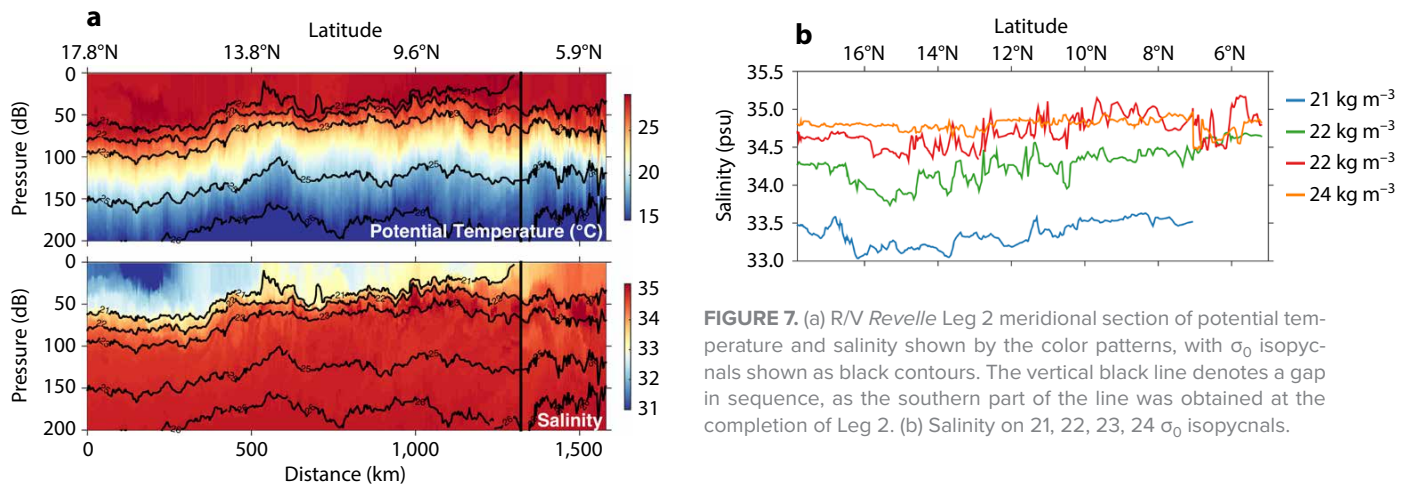


**FIGURE 7.** (a) R/V *Revelle* Leg 2 meridional section of potential temperature and salinity shown by the color patterns, with  $\sigma_0$  isopycnals shown as black contours. The vertical black line denotes a gap in sequence, as the southern part of the line was obtained after the completion of Leg 2. (b) Salinity on 21, 22, 23, 24  $\sigma_0$  isopycnals.

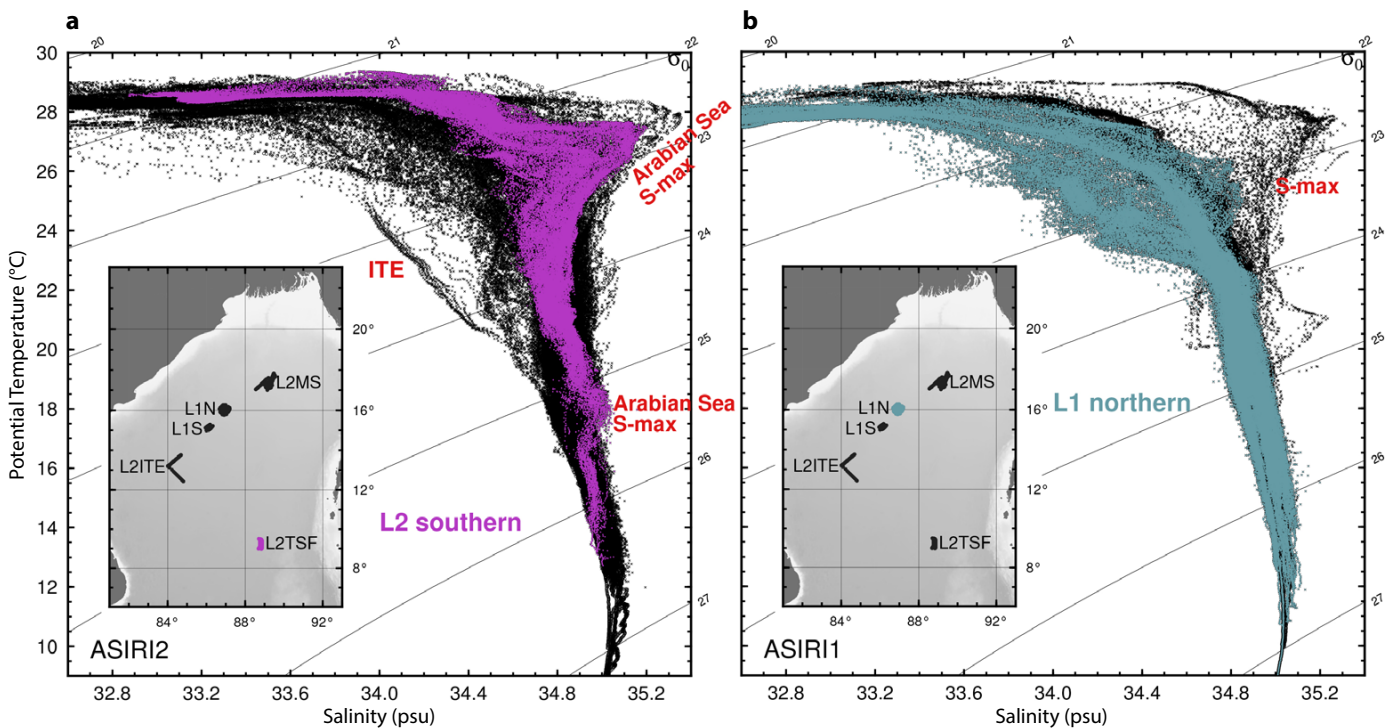


**FIGURE 8.** (a) Mesoscale feature “L2 southern” near 8.6°N is shown in purple over the full R/V *Revelle* Leg 2 T/S scatter in black dots. The ITE is the low-salinity feature between 20° and 26°C. (b) A northern mesoscale feature, “L1 northern,” is shown in “blue” over the full R/V *Revelle* Leg 1 T/S scatter in black dots.

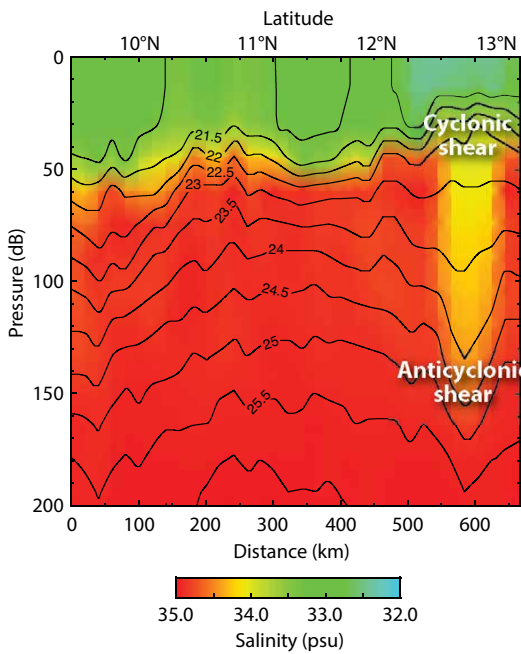


**FIGURE 9.** Intrathermocline eddy (see Figures 3a and 8 for position of the ITE) centered at 12.724°N, 84.515°E. Isopycnal contours are superimposed on the color salinity field.

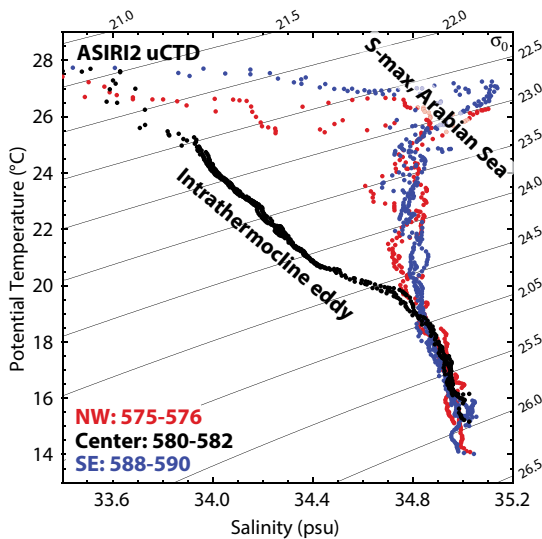


**FIGURE 10.** The T/S of the ITE core (black) and of the waters surrounding the ITE (red and blue).

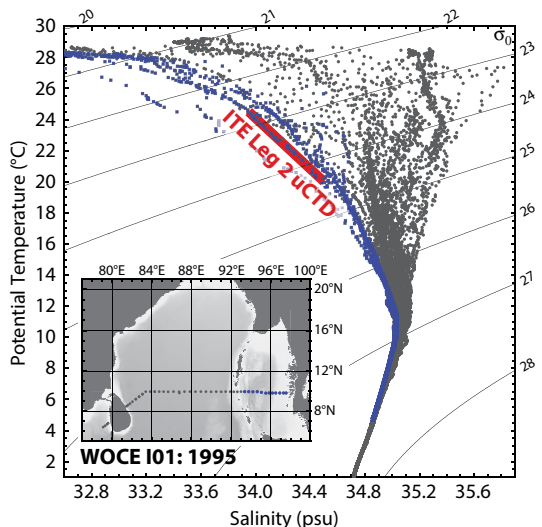


**FIGURE 11.** The WOCE I01 section (shown in Figure 1) T/S plot reveals ITE stratification in the eastern sector of the Bay of Bengal, mainly in the Andaman Sea.

thermocline forming a bowl (anticyclonic shear) defining the base of the lens. The temperature and salinity properties of the ITE are often distinct from those of the regional thermocline, suggesting a remote origin. ITEs have been detected in numerous regions of the ocean (Kostianoy and Belkin, 1991). The ITE observed during Leg 2 fits the classic ITE description. It is seen as a relatively fresh, nearly homogenous layer (Figure 9). The isopycnals deepen at the base and are uplifted at the crown, marking anticyclonic and cyclonic geostrophic shear, respectively. The geostrophic current relative to 200 decibars (not shown here), marking the base of the ITE, shows a maximum current of  $\sim 0.25 \text{ m s}^{-1}$  at 70–80 m depth. The surface current is about 50% of the subsurface  $v_{\text{max}}$ .

The T/S characteristics within the 22°C–26°C core of the ITE are not seen in any of the other Leg 1 or Leg 2 CTD data, but are common in the Argo data (Figure 6b), mainly to the east of the *Revelle* sampling region. Along the edges of the ITE there is a sharp T/S contrast with the ITE core water (Figure 10), as the AS  $S_{\text{max}}$  near 70–100 m depth swirls around the ITE core. The WOCE section (Figure 11) finds ITE T/S characteristics in the eastern BoB, perhaps as far east as the Andaman Sea. It is proposed that the ITE travels westward from the eastern BoB, a common trait of the regional mesoscale features (Figures 4 and 5).

## CONCLUSIONS

Thermohaline stratification within the Bay of Bengal is one of sharp contrasts. Salty Arabian Sea water within the upper thermocline spreads largely as eddies under a barrier layer of surface water, whose buoyancy is maintained by massive input of freshwater. The ocean processes that mix these waters along and across density surfaces ultimately influence sea surface temperature and air-sea exchange via control on upper-ocean stratification. The observations obtained from R/V *Roger Revelle* in November and December 2013 reveal a complex array of energetic mesoscale and submesoscale features, complete with swirls and fronts of contrasting temperature and salinity, as well as an ITE that obscures the regional pattern of the Bay of Bengal as visualized by Argo-based climatology. A general westward migration of mesoscale features is suggested that injects T/S characteristics from as far east as the Andaman Sea into the western Bay of Bengal. 🌐

## REFERENCES

- Akhil, V.P., F. Durand, M. Lengaigne, J. Vialard, M.G. Keerthi, V.V. Gopalakrishna, C. Deltel, F. Papa, and C. de Boyer Montegut. 2014. A modeling study of the processes of surface salinity seasonal cycle in the Bay of Bengal. *Journal of Geophysical Research* 119:3,926–3,947, <http://dx.doi.org/10.1002/2013JC009632>.
- Bonjean, F., and G.S.E. Lagerloef. 2002. Diagnostic model and analysis of the surface currents in the tropical Pacific Ocean. *Journal of Physical Oceanography* 32:2,938–2,954, [http://dx.doi.org/10.1175/1520-0485\(2002\)032<2938:DMAAOT>2.0.CO;2](http://dx.doi.org/10.1175/1520-0485(2002)032<2938:DMAAOT>2.0.CO;2).
- Dugan, J.P., R. Mied, P. Mignerey, and A. Schuetz. 1982. Compact, intrathermocline eddies in the Sargasso Sea. *Journal of Geophysical Research* 87:385–393, <http://dx.doi.org/10.1029/JC087iC01p00385>.
- Durack, P.J., and S.E. Wijffels. 2010. Fifty-year trends in global ocean salinities and their relationship to broad-scale warming. *Journal of Climate* 23:4,342–4,362, <http://dx.doi.org/10.1175/2010JCLI33771>.
- Durand, F., D. Shankar, F. Birol, and S.S.C. Shenoi. 2009. Spatiotemporal structure of the East India Coastal Current from satellite altimetry. *Journal of Geophysical Research* 114, C02013, <http://dx.doi.org/10.1029/2008JC004807>.
- Gadgil, S., P.V. Joseph, and N.V. Joshi. 1984. Ocean-atmosphere coupling over monsoon regions. *Nature* 312:141–143, <http://dx.doi.org/10.1038/312141a0>.
- Gordon, A.L. 2001. Inter-ocean exchange. Pp. 303–314 in *Ocean Circulation and Climate*. G. Siedler, J. Church, and J. Gould, eds, Academic Press.
- Jensen, T.G. 2001. Arabian Sea and Bay of Bengal exchange of salt and tracers in an ocean model. *Geophysical Research Letters* 28:3,967–3,970, <http://dx.doi.org/10.1029/2001GL013422>.
- Jensen, T.G., H.W. Wijesekera, E.S. Nyadjro, P.G. Thoppil, J.F. Shriver, K.K. Sandeep, and V. Pant. 2016. Modeling salinity exchanges between the equatorial Indian Ocean and the Bay of Bengal. *Oceanography* 29(2):92–101, <http://dx.doi.org/10.5670/oceanog.2016.42>.
- Kostianoy, A.G., and I.M. Belkin. 1991. A survey of observations on intrathermocline eddies in the world ocean. Pp. 821–841 in *Mesoscale/Synoptic Coherent Structures in Geophysical Turbulence*. B.M. Jamart and J.C.J. Nihoul, eds, Elsevier.
- Lagerloef, G., F.R. Colomb, D. Le Vine, F. Wentz, S. Yueh, C. Ruf, J. Lilly, J. Gunn, Y. Chao, A. deCharon, G. Feldman, and C. Swift. 2008. The Aquarius/SAC-D Mission: Designed to meet the salinity remote-sensing challenge. *Oceanography* 21(1):68–81, <http://dx.doi.org/10.5670/oceanog.2008.68>.
- Pant, V., M.S. Girishkumar, T.V.S. Udaya Bhaskar, M. Ravichandran, F. Papa, and V.P. Thangaprakash. 2015. Observed interannual variability of near-surface salinity in the Bay of Bengal. *Journal of Geophysical Research* 120:3,315–3,329, <http://dx.doi.org/10.1002/2014JC010340>.
- Papa, F., F. Durand, W.B. Rossow, A. Rahman, and S.K. Bala. 2010. Satellite altimeter-derived monthly discharge of the Ganga-Brahmaputra River and its seasonal to interannual variations from 1993 to 2008. *Journal of Geophysical Research* 115, C12013, <http://dx.doi.org/10.1029/2009JC006075>.
- Rao, R.R., and R. Sivakumar. 2003. Seasonal variability of sea surface salinity and salt budget of the mixed layer of the north Indian Ocean. *Journal of Geophysical Research* 108(C1), 3009, <http://dx.doi.org/10.1029/2001JC000907>.
- Reynolds, R.W., T.M. Smith, C. Liu, D.B. Chelton, K.S. Casey, and M.G. Schlax. 2007. Daily high-resolution blended analyses for sea surface temperature. *Journal of Climate* 20:5,473–5,496, <http://dx.doi.org/10.1175/2007JCLI18241>.
- Sastry, J., D. Rao, V. Murty, Y. Sarma, A. Suryanarayana, and M. Babu. 1985. Watermass structure in the Bay of Bengal. *Mahasagar Bulletin of the National Institute of Oceanography* 18(2):153–162, <http://www.ijs.nio.org/index.php/msagar/article/view/1811>.
- Schott, A.F., and J. McCreary. 2001. The monsoon circulation of the Indian Ocean. *Progress in Oceanography* 51:1–123, [http://dx.doi.org/10.1016/S0079-6611\(01\)00083-0](http://dx.doi.org/10.1016/S0079-6611(01)00083-0).
- Schott, F.A., S.-P. Xie, and J.P. McCreary Jr. 2009. Indian Ocean circulation and climate variability. *Reviews of Geophysics* 47, RG1002, <http://dx.doi.org/10.1029/2007RG000245>.
- Sengupta, D., G.N. Bharath Raj, and S.S.C. Shenoi. 2006. Surface freshwater from Bay of Bengal runoff and Indonesian Throughflow in the tropical Indian Ocean. *Geophysical Research Letters* 33, L22609, <http://dx.doi.org/10.1029/2006GL027573>.
- Mahadevan, A., T. Paluszkiwicz, M. Ravichandran, D. Sengupta, and A. Tandon. 2016. Introduction to the special issue on the Bay of Bengal: From monsoons to mixing. *Oceanography* 29(2):14–17, <http://dx.doi.org/10.5670/oceanog.2016.34>.
- Shankar, D., P.N. Vinayachandran, and A.S. Unnikrishnan. 2002. The monsoon currents in the north Indian Ocean. *Progress in Oceanography* 52:63–120, [http://dx.doi.org/10.1016/S0079-6611\(02\)00024-1](http://dx.doi.org/10.1016/S0079-6611(02)00024-1).
- Shetye, S.R., A.D. Gouveia, D. Shankar, S.S.C. Shenoi, P.N. Vinayachandran, D. Sundar, G.S. Michael, and G. Nampoothiri. 1996. Hydrography and circulation in the western Bay of Bengal during the northeast monsoon. *Journal of Geophysical Research* 101(C6):14,011–14,025, <http://dx.doi.org/10.1029/95JC03307>.
- Shetye, S.R., S.S.C. Shenoi, A.D. Gouveia, G.S. Michael, D. Sundar, and N. Nampoothiri. 1991. Wind-driven coastal upwelling along the western boundary of the Bay of Bengal during the southwest monsoon. *Continental Shelf Research* 11:1,397–1,408, [http://dx.doi.org/10.1016/0278-4343\(91\)90042-5](http://dx.doi.org/10.1016/0278-4343(91)90042-5).
- Sprintall, J., G. Siedler, and H. Mercier. 2013. Inter-ocean and interbasin exchanges. Chapter 19 in *Ocean Circulation & Climate: A 21st Century Perspective*, 2nd ed. G. Siedler, S. Griffies, J. Gould, and J. Church, eds, Academic Press.
- Talley, L.D. 2013. *Hydrographic Atlas of the World Ocean Circulation Experiment (WOCE): Vol. 4. Indian Ocean*. M. Sparrow, P. Chapman, and J. Gould, series eds, International WOCE Project Office, Southampton, UK, 20 pp.
- Varkey, M.J., V.S.N. Murty, and A. Suryanarayana. 1996. Physical oceanography of the Bay of Bengal and Andaman Sea. *Oceanography and Marine Biology: An Annual Review* 34:1–70.
- Vinayachandran, P.N., Y. Masunoto, T. Mikawa, and T. Yarnagata. 1999. Intrusion of the Southwest Monsoon Current into the Bay of Bengal. *Journal of Geophysical Research* 104:11,077–11,085, <http://dx.doi.org/10.1029/1999JC900035>.
- Vinayachandran, P.N., V.S.N. Murty, and V. Ramesh Babu. 2002. Observations of barrier layer formation in the Bay of Bengal during summer monsoon. *Journal of Geophysical Research* 107(C12), 8018, <http://dx.doi.org/10.1029/2001JC000831>.
- Vinayachandran, P.N., D. Shankar, S. Vernekar, K.K. Sandeep, P. Amol, C.P. Neema, and A. Chatterjee. 2013. A summer monsoon pump to keep the Bay of Bengal salty. *Geophysical Research Letters* 40:1,777–1,782, <http://dx.doi.org/10.1002/grl.50274>.
- Wijesekera, H.W., T.G. Jensen, E. Jarosz, W.J. Teague, E.J. Metzger, D.W. Wang, S.U.P. Jinadasa, K. Arulananthan, L.R. Centurioni, and H.J.S. Fernando. 2015. Southern Bay of Bengal currents and salinity intrusions during the northeast monsoon. *Journal of Geophysical Research* 120:6,897–6,913, <http://dx.doi.org/10.1002/2015JC010744>.
- Wijesekera, H.W., E. Shroyer, A. Tandon, M. Ravichandran, D. Sengupta, S.U.P. Jinadasa, H.J.S. Fernando, N. Agarwal, K. Arulananthan, G.S. Bhat, and others. In press. ASIRI: An ocean-atmosphere initiative for the Bay of Bengal. *Bulletin of the American Meteorological Society*, <http://dx.doi.org/10.1175/BAMS-D-14-00197.1>.
- Wilson, E.A., and S.C. Riser. 2016. An assessment of the seasonal salinity budget for the upper Bay of Bengal. *Journal of Physical Oceanography* 46(5):1,361–1,376, <http://dx.doi.org/10.1175/JPO-D-15-01471>.
- Wyrtki, K. 1971. Oceanographic Atlas of the International Indian Ocean Expedition. National Science Foundation, OCE/NSF 86-00-001, Washington, DC, 531 pp.
- Yu, L., J.J. O'Brien, and J. Yang. 1991. On the remote forcing of the circulation in the Bay of Bengal. *Journal of Geophysical Research* 96(C11):20,449–20,454, <http://dx.doi.org/10.1029/91JC02424>.

## ACKNOWLEDGMENTS

We acknowledge Captain Tom Desjardins and the crew of R/V *Revelle* for their support in the collection of a remarkable data set. Support for Bay of Bengal research is provided by the Office of Naval Research. ALG award number N00014-14-10065. Lamont-Doherty Earth Observatory contribution number 8013. AM and MF award number N00014-13-10451 and for MF a WHOI summer student fellowship. ES award number N00014-14-10236.

## AUTHORS

**Arnold L. Gordon** (agordon@ldeo.columbia.edu) is Professor, Lamont-Doherty Earth Observatory of Columbia University, Palisades, NY, USA. **Emily L. Shroyer** is Assistant Professor, College of Earth, Ocean, and Atmospheric Sciences, Oregon State University, Corvallis, OR, USA. **Amala Mahadevan** is Senior Scientist, Woods Hole Oceanographic Institution, Woods Hole, MA, USA. **Debasis Sengupta** is Associate Professor, Centre for Atmospheric and Oceanic Sciences, Indian Institute of Science, Bangalore, India. **Mara Freilich** is a graduate student in the MIT/WHOI Joint Program in Oceanography, Cambridge/Woods Hole, MA, USA.

## ARTICLE CITATION

Gordon, A.L., E.L. Shroyer, A. Mahadevan, D. Sengupta, and M. Freilich. 2016. Bay of Bengal: 2013 northeast monsoon upper-ocean circulation. *Oceanography* 29(2):82–91, <http://dx.doi.org/10.5670/oceanog.2016.41>.